Special Topic Articles, JOURNAL OF PLASMA AND FUSION RESEARCH Vol. 93, No. 12, Dec. 2017.

Modeling of particle transport in the Magnetized Dusty Plasma Experiment

Edward Thomas, Jr.

Physics Department, Auburn University, Auburn, Alabama, U.S.A.
etjr@auburn.edu

(Accepted:)

Abstract:
For over a decade, it has been postulated that the addition of a magnetic field can have a profound influence on the properties of a complex/dusty plasma and a number of experimental devices have been built around the world to explore the physics of dusty plasmas in strongly magnetized plasmas. Just over two years ago, the Magnetized Dusty Plasma Experiment (MDPX) device at Auburn University became the latest facility commissioned to study dusty plasmas in strongly magnetized plasmas. In recent experimental observations, it has been shown that at magnetic fields above $|\boldsymbol{B}|$ = 1.5 T, the charged dust particles can form spatial pattern in the plasma that is identical to the spatial structure of a wire mesh at the boundary of the plasma. This paper discusses the results of numerical simulations that show qualitatively good agreement with the observation of semi-discrete particle motion in this imposed, ordered structure.

Keywords: magnetized dusty plasma, complex plasma, transport,

1. Introduction:

Dusty plasmas are four-component plasma systems consisting of electrons, ions, neutral atoms, and charged, solid "dust" particles. In typical laboratory experiments, these dust particles can range in size from 0.5 to 10 micrometers in diameter. The key feature of a dusty plasma is that these microparticles acquire a net charge from the surrounding plasma through the collection of electrons and ions. This net dust particle charge, q_d, is typically negative and can be several hundred to several thousand of elementary charges. However, due to the large mass of the microparticles, compared to the electrons and ions, the charge-to-mass ratio of a micron-sized dust particle can be a factor of 10^{-11} to 10^{-12} relative to the charge-to-mass ratio of an electron.

For the last three decades of dusty plasma research, there have only been a few experimental devices that have attempted to investigate the influence of magnetic fields on charged dust particles in a plasma. The small charge-to-mass ratio of the dust particles is the one of the important reasons for this. The Hall parameter, which is defined as the ratio of the cyclotron frequency to a collision frequency, is often used to describe the degree of magnetization of a system [1, 2]. For the dusty plasmas, the Hall parameter is given by:

$$H = \frac{\omega_{cd}}{\nu_{nd}} = \frac{q_d B}{m_d}\left(\frac{3m_d}{4\gamma\pi m_n v_{tn} N a^2}\right) \sim \frac{q_d B}{Na^2} \sim \frac{B}{aP} \quad (1)$$

Here, ω_{cd} is the dust cyclotron frequency given by the product of the dust grain charge and the magnetic field divided by the dust grain mass, m_d. ν_{nd} is the dust-neutral collision frequency which is derived from the Epstein drag - the drag force on a spherical object moving through a neutral gas – and which contains a geometric factor, $\gamma \sim 1$, the mass of the neutral atoms, m_n, the velocity of the neutral atoms, v_{tn}, the neutral gas number density, N, the radius of the dust particles, a, and the dust grain mass, m_d. It is assumed that the dust grains are electrically floating objects that act as spherical capacitors and therefore, the dust grain charge will scale linearly with the grain radius, $q_d = 4\pi\varepsilon_0 a\varphi$, where ε_0 is the permittivity of free space and φ is the surface potential of the dust grain. Since the neutral gas number density, N is directly proportional to the neutral gas pressure, P, the Hall parameter can be rescaled in terms of three experimental parameters, the magnetic field, the dust particle radius, and the neutral pressure.

It is concluded that in order to observe magnetic field effects in dusty plasmas, experiments need to be operated at a combination of large magnetic fields, small particle sizes, and low neutral pressures. In order to retain the ability to directly visualize micron-sized particles, the Hall parameter criterion requires

experiments to be performed at magnetic fields, $B \geq 1$ T for pressures $P < 10$ Pa. This is an experimentally challenging regime, often requiring the development of a superconducting magnetic field system along with new diagnostic tools to characterize the plasma and dusty plasma. Over the last decade, there have been few experiments that have sought to understand how the dusty plasmas are influenced by the magnetic field in Japan [3], Russia [4], and several experiments in Germany at the Max Planck Institute [5] and Kiel University [6, 7].

In this paper, an analysis of experimental results from the recently commissioned Magnetized Dusty Plasma Experiment (MDPX) device in the United States will be presented. Recent studies using the MDPX device have reported on the observation of a new type of imposed, ordered structure formed in the plasma at high magnetic field. One feature of this structure is the quasi-discrete, stepwise motion of the particles through this ordered structure [8]. In this paper, a single particle numerical simulation has been developed to model this stepwise motion. It will be shown that there is good qualitative agreement between the model and the experimental observations. This work motivates the development of a more complex, multi-particle model that will be described at the end of this paper.

The paper is organized as follows. Sec. 2 will describe the MDPX device and the experimental setup. Sec. 3 will describe the model and numerical results. Finally, Sec. 4 will present a brief discussion of the results and plans for future studies.

2. The MDPX device:

The Magnetized Dusty Plasma Experiment (MDPX) device is the latest experimental facility that has been built to study the physics of charged dust particles in magnetized plasmas and magnetized dusty plasmas that builds upon the designs and experiences of the previous magnetized dust experiments. The MDPX device is a flexible, high magnetic field research instrument with a mission to serve as an open access, multi-user facility for the dusty plasma and basic plasma research communities. The MDPX device is constructed from two main components: (a) the superconducting coil system used to generate the magnetic field and (b) an octagonal vacuum chamber that is inserted into the magnet and used for plasma experiments. A brief summary of the MDPX design is given below. A more extensive description of the device is given in earlier papers [9, 10].

The magnet uses an "open bore" design concept with upper and lower cryostat sections that are separated by a 19 cm gap and a 50 cm diameter central warm bore that extends 157 cm axially. The cryostat contains a total of four superconducting coils, two in the upper half and two in the lower half. Because the coils can be independently controlled, the magnetic can be operated in several magnetic configurations including a highly uniform mode and a mode with a linear gradient of up to 2 T/m. The entire cryostat is mounted on a rotating support structure that allows us to perform experiments in configurations from the gravitational field and magnetic field aligned (i.e., $\boldsymbol{g} \parallel \boldsymbol{B}$) to the gravitational field and magnetic field oriented perpendicular to each other (i.e., $\boldsymbol{g} \perp \boldsymbol{B}$). The open bore concept means that when operating, experimenters have access to the central volume of the magnet from both the radial and axial directions, thereby maximizing the diagnostic access.

The primary vacuum chamber uses an octagonal design to provide four pairs of 127 mm tall × 102 mm wide access ports to the plasma volume. The chamber has an inner diameter of 356 mm, an outer diameter of 432 mm, and an interior (axial) height of 178 mm. Capacitively-coupled plasmas are generated using a pair of parallel plate electrodes 342 cm diameter electrodes using up to 10 W of 13.56 MHz radio frequency heating power, although experiments are typically performed using 1 to 3 W with one electrode powered and the other electrode either grounded or electrically floating, depending upon the experiment. The lower electrode has a 150 mm wide, 3.2 mm deep central depression to provide confinement for the dust particles. The upper electrode has a 146 mm through hole to allow viewing of the plasma volume. This through hole is generally covered by either a woven wire mesh or an ITO-coated glass plate.

Experiments described in this paper make use of a uniform magnetic field in the $\boldsymbol{g} \parallel \boldsymbol{B}$ configuration. The lower electrode was powered with 1.5 to 2.0 W of rf power and the upper electrode was electrically floating with the central hole covered by a wire mesh. The two electrodes were separated by 62 mm and a dusty plasma of 2.0 micron diameter particles was suspended ~20 mm above the lower electrode. Argon plasmas were generated with peak ion and electron densities (at $B = 0$ T and without dust) $n_i \approx n_e \sim 8 \times 10^{15}$ m^{-3} and an electron temperature, $T_e \sim 2$ eV with a neutral gas pressure, $P = 18$ Pa (135 mTorr). A schematic drawing of the electrode arrangement is shown in Fig. 1.

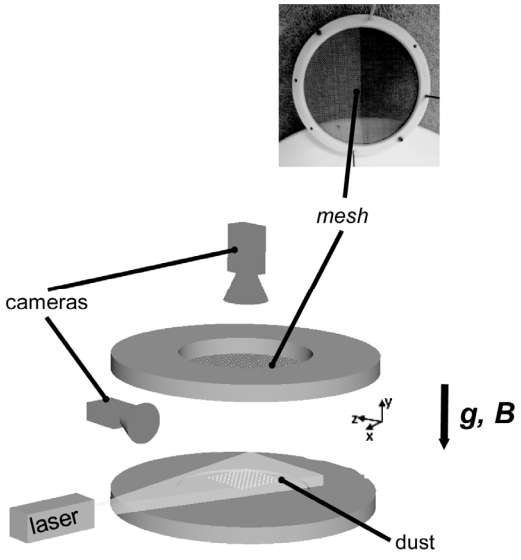

Fig. 1: Schematic drawing and photograph of the MDPX setup. The upper and lower electrodes are shown as is the location of the wire mesh. The dust particles are suspended in a layer above the lower electrode. For the experiments discussed in this work, the spacing between the electrodes was 62 mm. Images were recorded using the top camera.

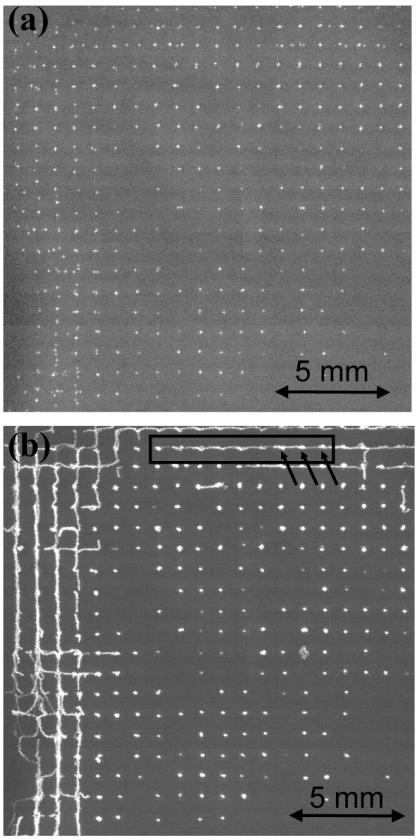

Fig. 2: (a) A single image that shows that regular, ordered structure formed by the particles suspended in the plasma. (b) A composite image consisting of the peak intensity from a combination of 100 video frames. The black box with the arrows shows the location of a particle that is moving from right to left. The arrows point to bright spots where the particle pauses in its motion. It is noted that the particles do not always pause in the motion. On the left side of the image, the particles are moving downward.

One of these observations was the formation of an ordered structure in the suspended dust particles that had the same spatial structure as the wire mesh when the experiment is operated at magnetic fields $|B| \geq 1.5$ T. This measurement was particularly surprising because the dust particles were suspended ~40 mm *below* the upper electrode. This distance is considerably larger than many of the characteristic plasma scale lengths of the plasma including: the electron Debye length (~0.3 mm), the ion-neutral mean free path (~1 mm) or the electron-neutral mean free path (~10 mm). Nonetheless, as shown in a single frame in Fig. 2(a) at $B = 2.5$ T, the spatial arrangement of the dust particles is quite uniform over an extended region of the particle cloud.

Fig. 2(b) shows a sum over 100 images recorded at 100 frames per second in order to reveal the motion of the particles. While most of the particles are fix in space, a few particles, such as those shown in the boxed region, are moving. The bright spots indicated by the arrows are locations where the particle motion is momentarily halted as the particles move in a stepwise fashion from one fixed point to another. Fig. 3 shows the measurement of the motion of a single particle. It is seen that the particle rapid moves from one fixed point to another and then remains momentarily trapped at a fixed point. This is a particle that is drifting from right to left (in the -*x*-direction). It is this type of motion that will be modeled in this paper.

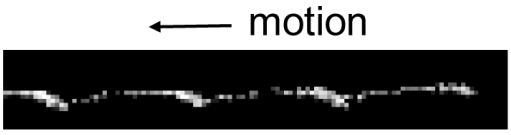

Fig. 3: An image of particle positions for a single particle that is moving in a quasi-discreet, stepwise fashion through the plasma. As in Fig. 2, the bright spots are places where the particle motion is nearly paused. The space between the brightest peaks matches the spatial structure of the wire mesh.

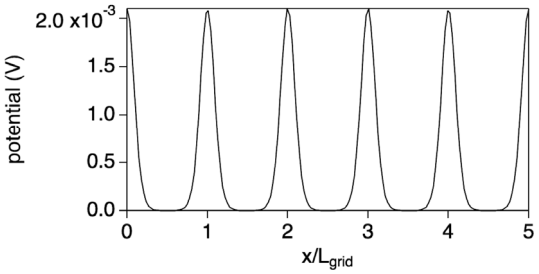

Fig. 4: Model of the trapping potential along the horizontal (x) direction. The parameters used for computing the potential are given in Table 1.

3. Model of the quasi-discrete particle motion

Although the detailed mechanisms that give rise to the imposed ordered structures (i.e., the dust gridding) remains unclear, it is still possible to develop a numerical model that allows the particle motion to be simulated and to make comparisons with the experimental measurements. While there are several free parameters, the model is guided by observations that have been made in MDPX and other high magnetic field dusty plasma experiments.

3.1 Development of the model

For the development of the model, six main criteria are considered.

1) The particles are restricted to moving in the x-y plane; that is, the simulated particles will be vertical equilibrium with gravity and will have a fixed charge;
2) The particles will be placed in a uniform magnetic field that is pointing in the – z-direction (into the page and parallel to the gravitational field), consistent with the experimental orientation of the MDPX device;
3) The grid structure will be modeled as localized, two-dimensional potential wells;
4) The particles will be subjected to a neutral drag force that is based upon the Epstein drag force that has been used extensively in dusty plasmas and described in detail in earlier papers [11 - 14];
5) The particles will be subjected to an azimuthal rotation that is driven by an ion $\boldsymbol{E}$ x $\boldsymbol{B}$ drift as observed in MDPX [15] and other magnetized dusty plasma experiment [3, 16, 17].
6) The particles are allowed to have a finite dust kinetic temperature;

For the criteria described above, items 1 and 2 establish the geometry of the model. For item 3, a functional form of the grid trapping potential was created and given in Eq. (2), below:

$$\varphi_{trap}(x,y) = A\left\{\exp\left[\frac{\cos\left(k_{grid}x\right)}{\sigma}\right] + \exp\left[\frac{\cos\left(k_{grid}y\right)}{\sigma}\right]\right\} \qquad (2)$$

The values of A, σ, and k_{grid} are chosen to satisfy two criteria: (a) that the depth of the potential well is $\varphi \sim 2$ mV (or about 5 times larger than the effective potential shown in Fig. 9 of Ref. [8]) and (b) that $k_{grid} = 2\pi/L_{grid}$, where L_{grid} is the center-to-center wire spacing of the mesh. The electric force on the particles is then computed from: $\vec{F}_{elec} = -q_d \nabla \varphi_{trap}$. Model of the trapping potential along the horizontal (x) direction is shown in Fig. 4.

For item 5, the ion drag force, the functional form given in Eq. (3) is used. This form is chosen to provide an *ad hoc* force in the azimuthal ($\hat{\varphi}$) vector direction to simulate the effect of the momentum transfer from the ions to the dust particles.

$$\vec{F}_{rot} = \alpha\left(\frac{r}{r_c}\right)\hat{\varphi} \qquad (3)$$

Tab. 1: Parameters used in the MDPX particle motion model.

Particle parameters:	
Diameter, $2a$	2.0 μm
Charge, q_d	5200 e^-
Mass, m_d	9.2 x 10^{-15} kg
Plasma parameters:	
Electron temperature, T_e	3 eV
Ion temperature, T_i	1/40 eV
Plasma number density, n	3 x 10^{15} m^{-3}
Gas species	Argon
Neutral pressure, P	13.3 Pa (100 mTorr)
Model Parameters:	
Grid spacing, L_{grid}	0.84 mm
Magnetic field, B	2.0 T
Width parameters, σ	0.3 m/s
Amplitude, A	6 x 10^{-5} V
Circulation parameter, α	8 x 10^{-16} N

Here, α is the strength of the force that is estimated from the taking the kinetic energy of a circulating dust grain and dividing by the radius of the circulation to define an effective force. In the simulation, $\alpha = 8 \times 10^{-16}$ N. In the simulation, r is measured from the center of the simulation region at $(x, y) = (0, 0)$ and r_c is a scaling parameter for the decay of the rotation which is set to $6*L_{grid}$.

For item 6, at each time step, the dust particles are given an additional random velocity to simulate the effect of a thermal distribution. This velocity is chosen from a Gaussian noise distribution function in such manner so that the velocity distribution of a fixed particle in the simulation is comparable to the velocity distribution shown in Fig. 7 of Ref. [8]. A summary of the parameters used in the simulation is given in Tab. 1.

The single particle motion is simulated using a Newton solver. The particles are assumed to move with a constant acceleration over a small time step that is $\Delta t \sim 1$ μsec. Using the criteria defined above, a generalized equation of motion, Eq. (4), can be solved to determine the dynamics of the particle in the magnetic field. It is noted that for the particles of interest in this simulation, 2 micrometer diameters, silica particles, the last term is small compared to the other terms and so no direct magnetic effects (e.g., gyromotion) are expected to be observed in this simulation.

$$\vec{F} = m_d \frac{d\vec{v}_d}{dt} = \vec{F}_{cirl} + \vec{F}_{neutral-drag} + q_d \vec{E}_{trap} + q_d \vec{v}_d \times \vec{B} \tag{4}$$

3.2 Results from the model

Results from three different simulation cases are presented. In the first case, shown in Fig. 5, is an example of the stepwise motion observed in the simulation for a single particle for a simulated time of 10 seconds. In this case, the particle is started at the location $(x/L_{grid}, y/L_{grid}) = (8, 2)$. The particle is then moves from this initial position becoming "trapped" for short periods at various integer grid points, for example at positions (6,1), (5,4), (3,4), and (2,5). This result is generally consistent with the motion of the particles that is seen in Fig. 2(b). These results also show the general circulation of the particle in the plasma.

In recent studies on the MDPX device, it has been shown that the charge on the dust particle may be lower than the value estimated using the usual orbital-motion-limited charge model [18, 19]. Therefore, it was of interest to understand how variations in the dust grain charge could impact the stepwise motion of the particles. In this case, a comparison is performed of 400 different simulation runs in which the charge of the dust particle is varied. In each simulation, the particles have the same starting position, but the initial velocity is picked randomly from a Gaussian distribution. Each

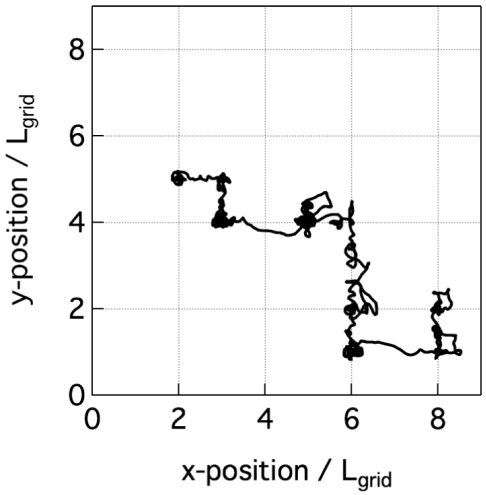

Fig. 5: Output from the single particle simulation that shows the stepwise motion of the particles as they move through the plasma. The particles start at (x/L_{grid}, y/L_{grid}) = (8, 2) and are generally moving in a counter-clockwise

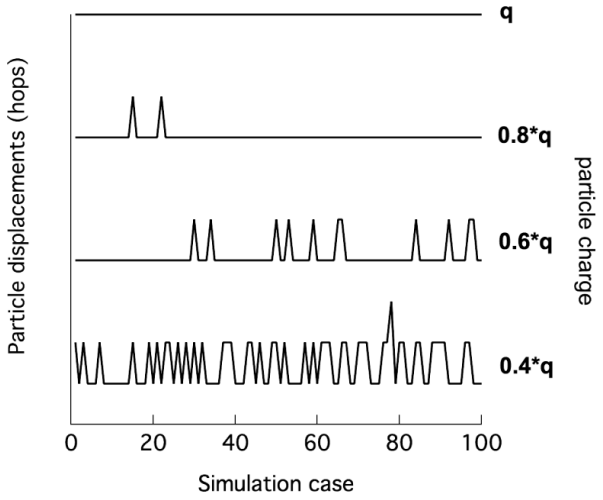

Fig. 6: Comparison of the quasi-discreet, stepwise motion as a function of the dust grain charge. Each line represents 100 simulation runs. The individual peaks in each curve indicate a specific run in which the particle has made one or more steps. The flat line for $q = q_0$ indicates that the particle was always trapped. Within decreasing particles charge, the strength of the electrostatic trap decreases and the particles become less confined.

simulation is run for 4 seconds of simulation time and the circulation force is not used. In the results shown in Fig. 6, each "peak" in the curve represents a simulation run in which the particle makes a stepwise displacement from its starting position. It is shown that with decreasing particle charge, the number of displacements will greatly increase. In comparison with the experiments, it is observed in Fig. 2(b) that parts of the particle cloud show fixed particles – mostly the central region – while the outer portion of the cloud shows movement.

The simulation assumes that the plasma conditions across the region where the particles are suspended is uniform. Because of the small size of the grid structure, L_{grid} = 0.84 mm, combined with the challenges of diagnosing the plasma at high magnetic field, it is difficult measure the plasma parameter. However, if there is some spatial variation in the plasma parameters, it could lead to a variation in the particle charge. Therefore, the simulation results may provide a guide for considering how the particle charge may be varying.

The final simulation result is a qualitative comparison between the stepwise motion of the particles in the experiment and simulation. Fig. 7 shows an expanded view of the horizontal motion of a particle. In Fig. 7(a) the *x*-*y* trajectory of the particle is shown. The particle is moving from right to left and is shown to come to rest near $x_{norm} = x/L_{grid}$ = 3, 2, and 1. This is similar to the trajectory plot of a particle shown in Fig. 3. Fig. 7(b) shows the direct output from the simulation of the particle velocity as a function of the horizontal position. However, it was determined that this is not the best way to make a comparison with the experiment since the experimental data is recorded at 100 frames/second and a running average over 5 position measurements is used to obtain the velocity vs. position Therefore, to make a comparison between the experiment and the simulation, the simulation data is resampled every 0.01 seconds (i.e., at 100 Hz) and the position locations are used to compute the velocity using the same algorithm as the experimental data. This is presented in Fig. 7(c) and this figure should be compared with the equivalent experimental plot shown in Fig. 7(d).

4. Discussion

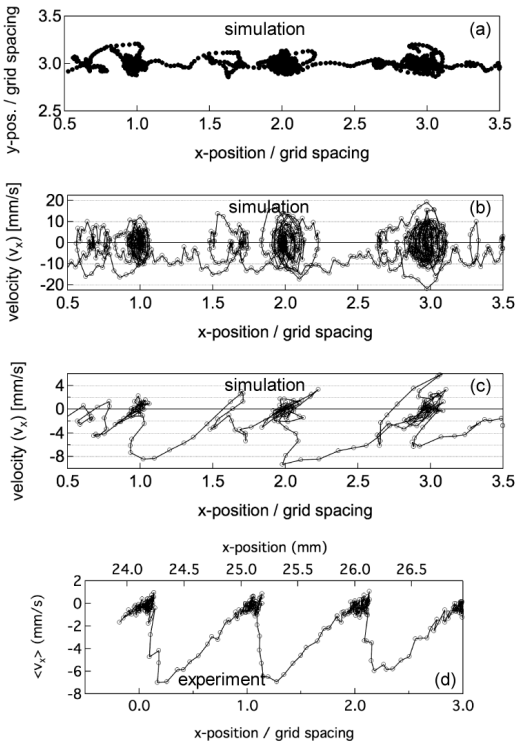

Fig. 7: (a) [Simulation] Plot showing the trajectory of a particle for three consecutive steps. (b) [Simulation] Plot of the output velocity of the particles as a function of spatial position. (c) [Simulation] Reprocessing of the velocity vs. position plot using a "camera" sampling rate of Δt = 0.01 s. (d) [Experiment] A velocity vs. position plot for a 2 micron diameter particle in the plasma.

While it is not yet possible to make a direct quantitative comparison between the experiment and simulation data, but it is already clear that the two results share many similarities and can provide some insights into the behavior of dust particles in the MDPX device. First, the simulations do show that it is possible to develop a model that can give qualitatively similar results as the experiment. While these results are limited by the fact that there is not a self-consistent description of the particle circulation, the use of a periodic structure of potential wells for trapping the particles does appear to be reasonable. Yet, it is clear that additional theoretical developments are needed to fully describe and understand how these potential structures are formed in the plasma.

A second important result is the possible role of particle charge in determining the observed dynamics. As stated in Sec. 3, there is growing evidence that the dust particle charge may be lower than had previously been anticipated. Since the trapping potential gives rise to an electric force on the particles, it is not surprising that the confinement of the particles becomes less effective with decreasing charge.

To continue this work, a more robust, multi-particle approach is needed. This initial work demonstrates that the form of the trapping potential is a reasonable starting point for a more advanced model. The next step will be to incorporate the trapping potential structure shown in our laboratory's molecular dynamics code [20] in order to perform to investigate the role of inter-particle interactions in the trapping behavior. However, this work does provide a good starting point for trying to understand the particle dynamics in the MDPX device.

Acknowledgements

This work is supported by research grants from the U.S. Department of Energy (DE-SC0016330) and the U.S. National Science Foundation (NSF-1613087). The author extends his thanks to the entire MDPX research team for their support.

References

[1] J. Carstensen, F. Greiner, and A. Piel, "Ion-Wake-Mediated Particle Interaction in a Magnetized-Plasma Flow," *Phys. Rev. Lett.*, **109**, 135001 (2012).

[2] E. Thomas, A. M. DuBois, B. Lynch, S. Adams, R. Fisher, D. Artis, S. LeBlanc, U. Konopka, R. L. Merlino, and M. Rosenberg, "Preliminary characteristics of magnetic field and plasma performance in the Magnetized Dusty Plasma Experiment (MDPX)," *J. Plasma Phys.*, **80**, 803 (2014).

[3] N. Sato, G. Uchida, T. Kaneko, S. Shimizu, and S. Iizuka, "Dynamics of fine particles in magnetized plasmas," *Phys. Plasmas*, **8**, 1786 (2001).

[4] M. M. Vasil'ev, L. G. D'yachkov, S. N. Antipov, O. F. Petrov, and V. E. Fortov, "Dusty plasma structures in magnetic fields in a dc discharge," *J. Exp. Theo. Phys. Lett.*, **86**, 358 (2007).

[5] M. Schwabe, U. Konopka, P. Bandyopadhyay, and G. E. Morfill, "Pattern Formation in a Complex Plasma in High Magnetic Fields," *Phys. Rev. Lett.*, **106**, 215004 (2011).

[6] S. Knist, F. Greiner, F. Biss, and A. Piel, "Influence of Negative Ions on Drift Waves in a Low-Density Ar/O2-Plasma," *Contrib. Plasma Phys.*, **51**, 769 (2011).

[7] B. Tadsen, F. Greiner, and A. Piel, "Preparation of magnetized nanodusty plasmas in a radio frequency-

driven parallel-plate reactor," *Phys. Plasmas*, **21**, 103704 (2014).
[8] E. Thomas Jr, U. Konopka, B. Lynch, S. Adams, S. LeBlanc, R. L. Merlino, and M. Rosenberg, "Quasi-discrete particle motion in an externally imposed, ordered structure in a dusty plasma at high magnetic field," *Phys. Plasmas*, **22**, 113708 (2015).
[9] C. E. Miller, A. Radovinsky, and S. Pourrahimi, "Structural Analyses of the Cold Mass for High Field Dusty Plasma Experiment," *IEEE Transactions on Applied Superconductivity*, **24**,1 (2014).
[10] E. Thomas, U. Konopka, D. Artis, B. Lynch, S. LeBlanc, S. Adams, R. L. Merlino, and M. Rosenberg, "The magnetized dusty plasma experiment (MDPX)," *J. Plasma Phys.*, **81**, 345810206 (2015).
[11] P. Epstein, "On the Resistance Experienced by Spheres in their Motion through Gases," *Physical Review*, **23**, 710 (1924).
[12] A. Piel and A. Melzer, "Dynamical processes in complex plasmas," *Plasma Phys. Control. Fusion*, **44**, R1 (2002).
[13] Bin Liu, J. Goree, V. Nosenko, and L. Boufendi, "Radiation pressure and gas drag forces on a melamine-formaldehyde microsphere in a dusty plasma," *Phys. Plasmas*, **10**, 9 (2003).
[14] M. Puttscher and A. Melzer, "Dust particles under the influence of crossed electric and magnetic fields in the sheath of an rf discharge," *Phys. Plasmas*, **21**, 123704, (2014).
[15] E. Thomas Jr, U. Konopka, R. L. Merlino, and M. Rosenberg, "Initial measurements of two- and three-dimensional ordering, waves, and plasma filamentation in the Magnetized Dusty Plasma Experiment," *Phys. Plasmas*, **23**, 055701 (2016).
[16] U. Konopka, D. Samsonov, A. Ivlev, and J. Goree, "Rigid and differential plasma crystal rotation induced by magnetic fields," *Phys. Rev. E*, **61**, 1890 (2000).
[17] P. K. Kaw, K. Nishikawa, and N. Sato, "Rotation in collisional strongly coupled dusty plasmas in a magnetic field," *Phys. Plasmas*, **9**, 387 (2002).
[18] M. Puttscher, A. Melzer, U. Konopka, S. LeBlanc, B. Lynch, and E. Thomas Jr, "Vertical oscillations of dust particles in a strongly magnetized plasma sheath induced by horizontal laser manipulation," *Phys. Plasmas*, **24**, 013701 (2017).
[19] Brian Lynch, Ph.D. Dissertation, "Microparticle Dynamics in Strongly Magnetized Low Temperature Plasmas", Auburn University, 2017.
[20] R. A. Jefferson, R. Jefferson, M. Cianciosa, and E. Thomas, "Simulations of one- and two-dimensional complex plasmas using a modular, object-oriented code," *Phys. Plasmas*, **17**, 113704 (2010).

Author information:

Prof. Edward Thomas, Jr. is the Charles W. Barkley and Lawrence C. Wit Professor of Physics at Auburn University, Auburn, Alabama, USA. Prof. Thomas completed a Bachelor's degree at the Florida Institute of Technology, a Master's degree at the Massachusetts Institute of Technology, and a Ph.D. at Auburn University. His research interests are in the areas of experimental and computational plasma physics with a particular focus on studies of dusty plasmas. He is currently supported by NASA, NSF, and the U.S. Department of Energy. He is a member of the International Union of Radio Science (URSI), University Fusion Association, and a Fellow of the American Physical Society.